Osteoarthritis and Cartilage

I C R S

International Cartilage Repair Society

OARSI — OSTEOARTHRITIS RESEARCH SOCIETY INTERNATIONAL

Perlecan in late stages of osteoarthritis of the human knee joint[1]

F. Tesche and N. Miosge*
This work is dedicated to the memory of Dr Rupert Timpl.
Zentrum Anatomie, Abteilung Histologie, Kreuzbergring 36, 37075 Göttingen, Germany

Summary

Objective: Disturbances of the proteoglycan metabolism play an essential role in the pathology of osteoarthritis. The extracellular matrix proteoglycan, perlecan, has lately been identified as a cell biological factor in cartilage development and maintenance. We investigated the tissue distribution of perlecan, the relation between the level of the protein and its mRNA and which type of cell, type 1 chondrocytes or elongated secretory type 2 cells, produces perlecan in late stages of osteoarthritis.

Methods: In 10 patients suffering from late-stage osteoarthritis tissue samples taken from a macroscopically intact area and the area adjacent to the main cartilage defect were investigated. We performed quantitative immunogold histochemistry and *in situ* hybridization *in vivo* and determined the level of perlecan mRNA with the help of real-time RT-PCR in native cartilage tissue and in cultured cells.

Results: *In vivo*, an increased level of perlecan protein was found in the area adjacent to the main defect. A 45% rise in the level of perlecan mRNA secreted by elongated secretory type 2 cells in comparison to type 1 chondrocytes was detected. Type 2 cells also translated the highest levels of perlecan to be deposited mainly in the pericellular matrix, and also in the interterritorial matrix in late stages of osteoarthritis. Also *in vitro*, type 2 cells showed a 50% higher level of mRNA for perlecan.

Conclusion: We found evidence that perlecan is involved in the pathogenesis of late stages of osteoarthritis. The levels of perlecan protein and mRNA are up-regulated especially by the elongated secretory type 2 cells in the area adjacent to the main cartilage defect. This might be seen as an attempt on the part of the cartilage tissue to stabilize the extracellular matrix.
© 2004 OsteoArthritis Research Society International. Published by Elsevier Ltd. All rights reserved.

Key words: Perlecan, Late-stage osteoarthritis, Human articular cartilage, Proteoglycan.

Introduction

Articular cartilage is a highly specialized connective tissue, which covers the articulating ends of long bones[1]. The resilience, integrity and function of articular cartilage are guaranteed by the content and organization of the abundant extracellular matrix composed of a system of collagen fibrils in which a network of proteoglycans is embedded[2]. The chondrocytes, responsible for production, organization and maintenance of the extracellular matrix, constitute only 5−10% of the tissue volume and lack direct cell−cell contacts[3,4].

Normal adult hyaline cartilage contains types II, VI, IX, X and XI collagen, the greatest amount being collagen type II[5]. Collagen types II, IX and XI form fibrillar alloys with type XI as core and collagen type IX on the outside possibly limiting the fiber diameter[1,6,7]. The other important cornerstones of the extracellular matrix are the proteoglycans. They all consist of a core protein containing one or more glycosaminoglycan side chains[8]. With reference to the nature of their core proteins it is possible to allocate each proteoglycan to one of the several classes[9], for example, large proteoglycans, such as aggrecan[10] and small proteoglycans such as fibromodulin, epiphycan, decorin and biglycan[9,11,12].

Perlecan, as a new member of the proteoglycans found in cartilage[13], is a large heparan sulfate proteoglycan present in all basement membranes[14]. It has been shown that perlecan is prominent in cartilage[9,13] and is enriched mainly in the pericellular environment of the chondrocytes[15,16], suggesting a role in the attachment of chondrocytes to their own matrix[13]. The perlecan core protein is involved in the control of important biological functions such as cell adhesion[17], maintenance of the extracellular matrix[18,19], binding to growth factors[20], cartilage development[21] and regulation of chondrocyte differentiation[22]. The perlecan gene encodes an approximately 467 kDa protein core consisting of five distinct domains. The N-terminal domain I is unique to perlecan, whereas domains II−V share sequence similarities with other cell surface and extracellular matrix proteins[23]. Domain I contains a cluster of three potential glycosaminoglycan attachment sites usually occupied by heparan sulfate side chains and may play an important role in chondrocyte differentiation and cartilage development[24]. Furthermore, mutations in perlecan lead to skeletal disorders. The relatively mild Schwartz−Jampel syndrome as well as the neonatal lethal dyssegmental dysplasia of the Silverman−Handmaker type show disorganization of the articular cartilage structure[15,25].

Up to the present, nothing is known about the role of perlecan in osteoarthritis (OA), but important biological functions of this proteoglycan have already been established and it is possible that perlecan is involved in the pathophysiology of this disease. OA is an almost universal, slowly progressive degenerative process, which may take years to develop. The centre of the pathogenesis of OA is

a disturbed cell−matrix relationship[26]. The primary lesion of the osteoarthritic process seems to be in the articular cartilage itself, i.e. to involve the chondrocytes and their surrounding matrix[27]. Further steps in the progress of this disease are the disruption of the matrix framework and the increasing water content followed by a loss of matrix strength[28]. A loss of the proteoglycans, aggrecan and decorin, collagen fiber fibrillation and surface splits occur in early stages of OA[26,29]. An initially increased production of collagen type II has been detected only in early disease stages[30]. In contrast, late stages of OA show a mixture of re- and degeneration processes[31,32]. One indication of this is the occurrence of three main types of chondrocytes, which have been identified in osteoarthritic cartilage at the ultrastructural level[33]. Type 1 chondrocytes show a typical chondrocyte phenotype and may be arranged in clusters. These cells are mainly found in the macroscopically intact area of osteoarthritic cartilage. The elongated secretory type 2 cells, which have an irregular shape with a prominent rough endoplasmic reticulum, are mainly found in the deep zones of articular cartilage of the areas adjacent to the main defect. Degenerative type 3 cells are mainly found in the main defect itself and undergo degradation[33−35]. At the more advanced stages of OA, elongated secretory type 2 cells express collagens, such as collagen types I and III[32,35] while the amounts of collagen type II are decreased[26]. The levels of transcription and translation for decorin and biglycan are also up-regulated in these cells[34]. Furthermore, fissures extending deep into the cartilage substance and cell cluster formation occur. These stages of disease are driven by degenerative processes catalyzed by tissue pro-teases[29,36], finally leading to the destruction of the articular cartilage with denudation of the subchondral bone[37].

In the present study, we investigated the levels of perlecan protein and mRNA and their distribution in the different chondrocyte cell types[33,34] of late-stage osteoarthritic cartilage from human knee joints. For *in vivo* analysis, we performed light and electron microscopic immunohistochemistry and *in situ* hybridization, as well as real-time RT-PCR to quantitate the level of mRNA. Furthermore, we isolated the two cell types from osteoarthritic tissue taken from the patients and cultivated them separately. We also applied real-time RT-PCR to quantitate the level of mRNA produced by these two cell types *in vitro*.

Materials and methods

TISSUE SAMPLES

Adult osteoarthritic articular cartilage was obtained from the knee joints of 10 patients (age range 63−79 years) undergoing an operation for a total knee arthroplasty. Tissue specimens were collected from a region directly adjacent to the main defect and from a macroscopically intact region at the lateral border of the joint. The patients were suffering from late-stage OA and all met the American College of Rheumatology classification criteria[38]. Healthy control cartilage from a 50-year-old accident victim was also investigated. Patients gave their written informed consent according to the Ethics Regulations of the Medical Faculty of the Georg-August University Goettingen.

TISSUE PREPARATION AND SECTIONING

Specimens of articular cartilage were fixed in a for-maldehyde solution, decalcified, dehydrated and finally embedded in paraffin for light microscopic investigations[39]. Afterwards, sections (4−5 μm) were cut and transferred onto slides. For topographical orientation and pathohistological grading, we stained the sections with Alcian blue and hematoxylin−eosin (H.E.). For electron microscopy, we exclusively investigated specimens from the radial zone adjoining the tidemark. Tissue samples (1 mm^3) were cut and fixed for 15 min in 4% paraformaldehyde and 0.5% glutaral-dehyde in phosphate-buffered saline (PBS) at 4°C. The tissue specimens were embedded in the hydrophilic resin LR-Gold® (London Resin Company, Reading, UK) as previously described[35]. Subsequently, ultrathin sections (80 nm) were cut and collected on formvar® coated nickel grids.

ANTIBODIES

Anti-DIG antibody (sheep IgG) was obtained from Quartett, Berlin, and an affinity-purified goat-anti-rabbit IgG from Medac, Hamburg. Each of them was coupled to 16 nm colloidal gold particles according to standard proto-cols[34]. Furthermore, we used an anti-DIG phosphatase-labeled antibody from Roche Diagnostics, Heidelberg, for light microscopic *in situ* hybridization and a well-character-ized, affinity-purified rabbit antibody against perlecan[17].

LIGHT AND ELECTRON MICROSCOPIC IMMUNOHISTOCHEMISTRY

We performed the peroxidase anti-peroxidase (PAP) method with DAB substrate as described previously[39] and applied the primary antibody against perlecan diluted 1:50 in 1% BSA/PBS at RT for 15 h. For electron microscopic immunogold histochemistry, the goat-anti-rabbit IgG was labeled with gold particles as previously described[34,35]. Ultrathin tissue sections were incubated with the anti-perlecan antibody diluted 1:50 in PBS for 1 h at RT. The secondary gold-coupled antibody, diluted 1:300 in PBS, was applied for 20 min at RT. Staining with uranyl acetate followed and reactions were examined with the help of a Zeiss EM 906E electron microscope.

CONTROLS

For the PAP method, negative controls were performed by treating the sections with 1% PBS/BSA instead of the primary antibody and by carrying out only the DAB reaction. For the control for the immunogold histochemistry the tissue samples were incubated with pure gold solution in order to exclude unspecific binding of free colloidal gold. Further-more, the reactions were performed with gold-coupled goat-anti-rabbit IgG to exclude non-specific IgG binding.

STATISTICAL ANALYSIS

Micrographs of the two different cell types from all patients ($n = 10$) were pooled. Mean values of the numbers of gold particles per cell (with s.e.m. ranging from 1 to 2) were analyzed in an area of 2000 nm^2 around 10 cells from each patient. Significant differences in the number of gold particles were noted for *P*-values ($P \leq 0.001$) using the Wilcoxon−Mann−Whitney test for unpaired samples.

PROBE PREPARATION

RNA was isolated as described below and re-verse transcribed into perlecan-specific cDNA. PCR was

performed with primers specific for perlecan and a T3-promoter sequence 5′-CAG AGA TGC AAT TAA CCC TCA CTA AAG GGC TCG GGG CGA ACT GAT GGT A-3′ (a reverse primer) and a T7-promoter sequence 5′-CCA AGC TTC TAA TAC GAC TCA CTA TAG GGA CCT TCG CTG GCT CAA GGA G-3′ (a forward primer) to insert the promoter sequences. Afterwards, *in vitro* transcription of non-radioactive sense and antisense RNAs with a digoxigenin labeling kit (Boehringer DIG-RNA labeling kit, Boehringer, Mannheim, Germany) was performed applying the T3- and T7-polymerases (Gibco/BRL, Heidelberg, Germany). Following extraction of the probes with phenol—chloroform these were precipitated with absolute ethanol and dissolved in DEPC—H$_2$O.

LIGHT AND ELECTRON MICROSCOPIC *IN SITU* HYBRIDIZATION

For light microscopic investigations, paraffin sections were deparaffinized, rehydrated and pre-treated with proteinase K. For the hybridization, the probe concentration was 100 ng digoxigenin-labeled antisense probe for perlecan in 100 μl hybridization solution (50% formamide, 5× SSC, 0.1 mg/μl yeast-RNA, 10 ng/μl probe) for each section. Hybridization was carried out for 16 h at 50°C. Posthybridization treatment included a washing procedure with 4× SSC (3 × 10 min, at 50°C), 2× SSC (1 × 15 min, at 60°C), 0.1× SSC (1 × 15 min, at 60°C) and 0.05× SSC (1 × 15 min, at 60°C). Afterwards the incubation with

Table I
Data of patients with advanced stages of osteoarthritis of the knee joint

Patient	Sex	Age	Height (cm)	Weight (kg)	Pain
1	Female	79	170	75	Rest + load
2	Female	63	165	84	Rest + load
3	Female	73	170	95	Rest + load
4	Male	75	168	78	Rest
5	Male	71	175	80	Load
6	Female	64	168	75	Rest + load
7	Female	68	170	73	Load
8	Female	67	148	57	Rest
9	Male	75	168	82	Load
10	Female	67	169	75	Rest + load
Mean values		70.2	167.1	77.4	

the anti-DIG phosphatase-labeled antibody diluted 1:300 in PBS was started. Finally color reactions were started with NBT/BCIP substrate. For electron microscopy, nickel grids were incubated with the same hybridization solution as described above for 19 h at 50°C. Probe concentration for perlecan was 100 ng digoxigenin-labeled antisense probe in 20 μl hybridization solution per grid. Rinsing steps were the same as described above. Afterwards, sections were incubated with the gold-coupled anti-DIG antibody in PBS (diluted 1:60) for 1 h at RT. The specimens were rinsed with PBS, contrasted and analyzed with the Zeiss EM 906E.

CONTROLS

Each hybridization was accompanied by a hybridization with an equivalently labeled amount of sense probe. Furthermore, hybridizations were performed without any RNA probes. Additionally, for the ultrastructural controls, tissue sections were treated with pure gold solution or the coupled anti-DIG antibody alone.

STATISTICAL ANALYSIS

For *in situ* hybridization at the ultrastructural level, micrographs of the two different cell types from patients ($n = 6$) were pooled and counted for gold particle contents. Mean values of the numbers of gold particles per cell (with S.E.M. ranging from 1 to 3) were analyzed in an area of 2000 nm^2 in 10 cells from each patient. Significant differences in the number of gold particles were noted for *P*-values ($P \leq 0.01$) using the Wilcoxon—Mann—Whitney test for unpaired samples.

CELL CULTURE

Two 0.5 cm^3 pieces of osteoarthritic cartilage tissue, one from an area adjacent to the main defect and one from a macroscopically intact area, from each of the four patients were minced and cells were isolated by treatment with collagenase type II (2 mg/ml, Sigma) in DMEM-F12 medium supplemented with 20% FSC and 100 μmol ascorbic acid overnight at 37°C and 5% CO$_2$. Thereafter, the suspension was centrifuged and the cells transferred to culture flasks coated with fibronectin in PBS (0.01 mg/25 cm^2). After a 10 h incubation period, the supernatant containing the type 1 chondrocytes was decanted into a new flask, while the elongated secretory type 2 cells already attached to the substratum remained in the first flask. After approximately
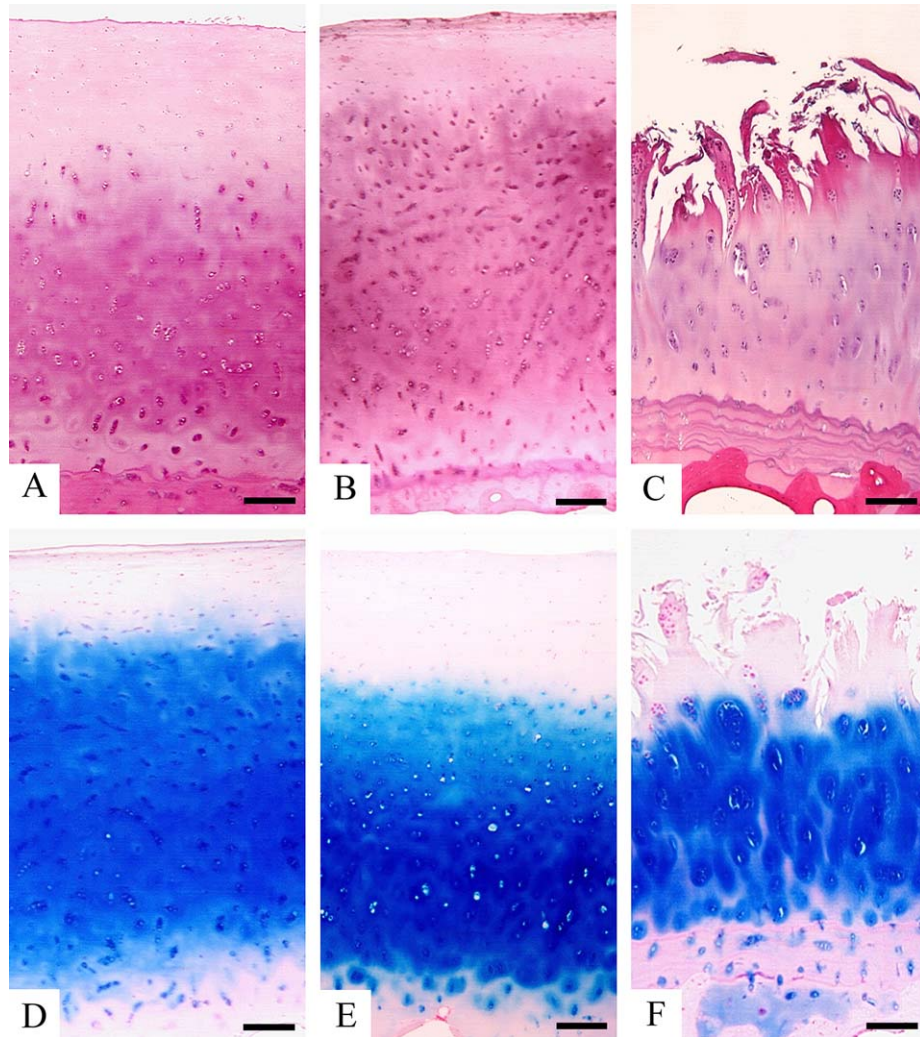

Fig. 1. Radiograph of a patient suffering from late-stage OA. Regions from which the tissue samples were taken are an area adjacent to the main defect (black arrow) and a macroscopically intact area (open arrow); bar = 2 cm.

Fig. 2. Histological evaluation of the cartilage samples with H.E. (A–C) and Alcian blue staining (D–F); bars = 70 μm. (A, D) Tissue samples from normal physiological cartilage with a homogeneously stained extracellular matrix. (B, E) Specimen taken from the macroscopically intact area of OA tissue. Note that only a few cells are arranged in clusters. (C, F) Cartilage samples from the area adjacent to the main defect. Note the increasing number of chondrocytes arranged in clusters, tidemark duplication, loss of the superficial zone, and the overall decreased Alcian blue staining with intense staining around the cell clusters.

2–3 weeks, when near confluence was reached, cells were harvested to isolate RNA.

RNA EXTRACTION FROM NATIVE CARTILAGE TISSUE

For the extraction of RNA from the native tissue, three cartilage tissue samples, each approximately 20 mg wet weight, were taken from each of three patients from the area adjacent to the main defect and from a macroscopically intact region at the lateral border of the joint and were frozen in liquid nitrogen, pulverised with a mortar and pestle, mixed in TRIZOL® (Biozol, Germany) and incubated for 10 min at RT. After a centrifugation step the aqueous phase was transferred to an RNAeasy Mini-column (RNAeasy Mini Kit, Qiagen) and processed according to the manufacturer's instructions.

RNA EXTRACTION FROM CULTURED CELLS AND RT

RNA from the cultured cells was isolated according to the manufacturer's instructions (RNAeasy Mini Kit, Qiagen); all RNA populations were treated with DNAfree® (Ambion) and reverse transcribed with the help of the Advantage RT-for-PCR Kit (BD Bioscience) applying MMLV reverse transcriptase and oligo(dT)$_{18}$ primer.

PCR

PCR conditions were optimized by applying the gradient function of the DNA engine Opticon 2 (MJ Research) for HPRT-1 (NM_000194)[40,41] and, for perlecan (M85289), primers (forward TCA GTC CCT TGT CAC CAT CCA, reverse TAA GCT GCC TCC ACG CTT AT) to amplify a 180 bp transcript were designed by the primer3® shareware. HPRT-1 was chosen as house-keeping gene because it has been described as being unregulated in many instances[40,41] and was proved to be unregulated particularly in our experimental setting. The PCR was performed in a total volume of 50 μl with 200 ng cDNA derived from the type 1 chondrocytes or the elongated secretory type 2 cells, 5 μl 10× reaction buffer, dNTP
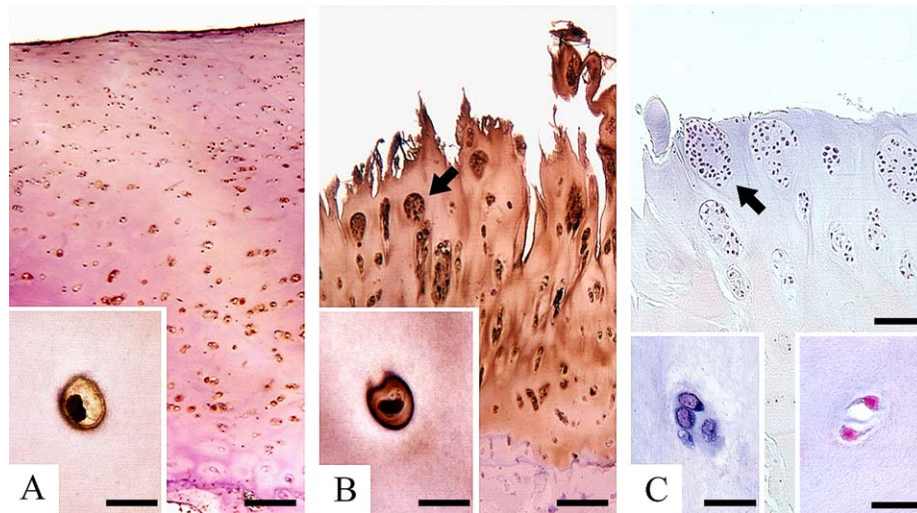
Fig. 3. Light microscopic immunohistochemistry (A, B) and *in situ* hybridization (C); bars = 70 μm, inset bars = 10 μm. (A) Staining for perlecan is detectable in the pericellular matrix around the cells from the radial zone and to a lesser extent from the cells of the transitional zone; inset: higher magnification of a chondrocyte from the radial zone. (B) Staining is more intense in the area adjacent to the main defect, especially in the surrounding matrix of chondrocytes arranged in clusters (arrow); inset: higher magnification of a chondrocyte from the radial zone. Furthermore, staining for perlecan is detectable in the interterritorial matrix. (C) Staining for perlecan mRNA (arrow) in chondrocytes arranged in clusters; left inset: higher magnification of a cluster with intense intracellular staining, right inset: control section with a sense probe.

10 μmol each, 20 pmol of each primer, 2.5 U hotstar *Taq* DNA polymerase (Qiagen) with the DNA engine Opticon 2 (MJ Research). After an initial activation step of 15 min at 95°C, further steps were as follows: 35 cycles of denaturing 30 s at 94°C, annealing 30 s at 61°C and elongation for 30 s at 72°C and, finally, extension for 10 min at 72°C. A total of 10 μl of each sample was loaded on a 1.5% agarose gel, and visualized by ethidium bromide after electrophoresis.

REAL-TIME PCR

In order to optimize the real-time PCR conditions for quantification, the optimal $MgCl_2$ concentration was determined. A total of 12.25 μl of $2\times$ QuantiTect SYBR Green PCR Master Mix (Qiagen), 20 pmol of each primer and 250 ng of cDNA were added to a final volume of 25 μl. Cycling was performed following the protocol described above. Data acquisition was carried out after each extension step and a melting curve was performed in 0.1°C steps from 50°C to 95°C. Real-time PCR efficiencies were calculated from the given slopes in Opticon 2 Monitor software[42]. Real-time PCR efficiency rates were high with values of 1.97. Experiments were performed four times in triplicate; the inter-test variation was ≤2.5% and the intra-test variation ≤1.2%. One PCR product was purified and sequenced to confirm that the nucleotide sequence was that of perlecan.

Results

PATIENT DATA

Macroscopically, all tissue samples from the patients revealed advanced OA with sclerosis and joint space narrowing (Fig. 1). Pathohistologically they could be classified as OA grades III–IV[43]. All patients suffered from load or rest-pain of the knee. No obvious correlation

between age, sex, weight, height, or clinical condition was detectable (Table I).

LIGHT MICROSCOPIC HISTOLOGY

The physiological normal control cartilage sections, obtained from a 50-year-old male accident victim, revealed a homogeneously stained matrix and a normal structure of articular cartilage following H.E. [Fig. 2(A)] and Alcian blue staining [Fig. 2(D)]. The specimens taken from the macroscopically intact cartilage areas of the patients with late-stage OA exhibited an increased number of cells, i.e. diffuse hypercellularity, and a small number of cells arranged in clusters [Fig. 2(B)]. Furthermore, reduced Alcian blue staining, indicating a loss of glycosaminoglycans, was detected [Fig. 2(E)]. The tissue samples from the area adjacent to the main defect revealed fissured cartilage tissue, an increased number of clusters [Fig. 2(C)] and reduced staining for Alcian blue [Fig. 2(F)].

LIGHT AND ELECTRON MICROSCOPIC IMMUNOHISTOCHEMISTRY

Light microscopic immunohistochemistry of the cartilage tissues revealed mainly pericellular staining for perlecan in all samples investigated. Specimens taken from the macroscopically intact areas [Fig. 3(A)] or from the healthy control cartilage (data not shown) showed strong staining in the pericellular matrix of the radial zone and weaker staining in the transitional zone. In contrast to the two zones described above, no staining for perlecan was detected in the superficial layer of articular cartilage. Furthermore, specimens taken from the area adjacent to the main defect revealed staining for the perlecan protein also in the interterritorial matrix and exhibited a more intense staining for perlecan than the specimens from the macroscopically

intact areas. The highest staining intensity was located in the surrounding matrix of chondrocytes organized in clusters [Fig. 3(B)]. Due to difficulties involved in differentiation between type 1 and type 2 cells at the light microscopic level we performed investigations at the ultrastructural level. Ultrastructurally, the macroscopically intact areas revealed chondrocytes of normal phenotype with sparse, finely structured endoplasmic reticulum. These type 1 cells with numerous filopodia were embedded in a homogeneous extracellular matrix with collagen fibers and proteoglycans [Fig. 4(A)]. The area adjacent to the main defect showed irregular, elongated cells containing large amounts of a prominent and enlarged rough endoplasmic reticulum [Fig. 4(B)] and was classified as elongated secretory type 2 cells[33,34]. In agreement with the results from the light microscopic immunohistochemistry we detected higher perlecan protein amounts at the ultrastructural level in the interterritorial matrix of the cartilage tissue samples taken from the area adjacent to the main defect where perlecan was found close to thin collagen fibers [Fig. 4(C)]. Similarly, immunogold histochemistry revealed staining for perlecan mainly in the extracellular matrix which directly surrounds the chondrocytes, i.e. the pericellular matrix, for type 1 cells [Fig. 5(A)] and type 2 cells [Fig. 5(B)]. The staining intensity was highest in the pericellular matrix of elongated secretory type 2 cells. Quantitation of the results of the immunogold histochemistry revealed a 20–30% higher amount of perlecan protein in the pericellular matrix surrounding the secretory type 2 cells as compared with the normal type 1 cells with P-values ≤ 0.001 [Fig. 6(A)].

CONTROLS

Neither the negative controls performed at the light microscopic level nor the control sections at the ultrastructural level incubated with pure gold solution or gold-coupled goat-anti-rabbit IgG revealed any reaction.

LIGHT AND ELECTRON MICROSCOPIC *IN SITU* HYBRIDIZATION

The cartilage samples investigated with light microscopic *in situ* hybridization exhibited an intracellular staining for perlecan mRNA in all specimens. As expected, only the nuclei of the chondrocytes and the extracellular matrix remained unstained. The tissue samples taken from the area adjacent to the main defect exhibited a more intensive staining than those taken from the macroscopically intact areas of articular cartilage from OA patients or healthy control cartilage (data not shown). A specimen from the area adjacent to the main defect is shown for perlecan mRNA staining in the cytoplasm of chondrocytes arranged in clusters [Fig. 3(C) and left inset]. Control hybridizations performed with an equivalent amount of sense probes remained negative [Fig. 3(C), right inset]. At the ultrastructural level, sparse staining for perlecan mRNA was detected in type 1 cells [Fig. 5(C)], while a greater number of gold particles were seen in the cytoplasm of type 2 cells [Fig. 5(D)]. Labeling was detected at the border of the rough endoplasmic reticulum in the cytoplasm of the chondrocytes classified as type 1 cells [Fig. 5(E)] and to a greater extent in type 2 cells [Fig. 5(F)]. Control hybridizations with sense probes were performed but neither for type 1 cells [Fig. 5(G)] nor for type 2 cells [Fig. 5(H)] was any staining detectable.
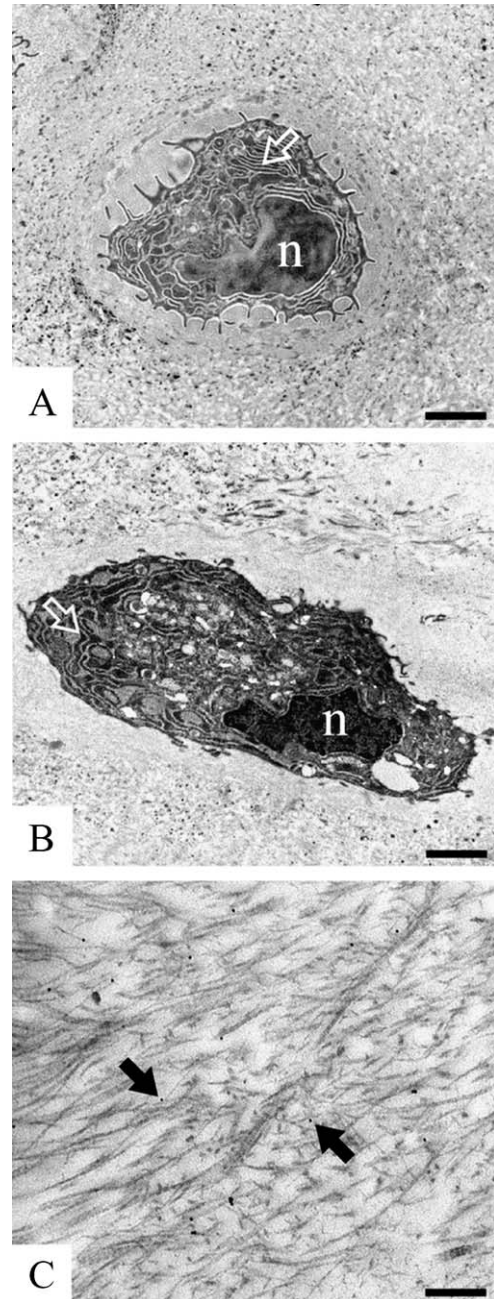

Fig. 4. Electron micrographs of the two different cell types (A, B) and the interterritorial matrix from a tissue sample taken from the area adjacent to the main defect (C). (A) Type 1 cell; note the round cell shape, the abundant filopodia and the fine endoplasmic reticulum (open arrow). (B) Type 2 cell; note the elongated cell shape, the sparse podofilia and the dilated endoplasmic reticulum (open arrow); n = nucleus, bars = 0.8 μm. (C) Immunogold histochemistry for perlecan protein. Staining is detectable in the interterritorial matrix close to thin collagen fibers (black arrows); bar = 0.3 μm.

Quantitation of the results of the ultrastructural *in situ* hybridization revealed an approximately 45% higher amount of perlecan mRNA in the elongated secretory type 2 cells than in the type 1 cells with P-values ≤ 0.01 [Fig. 6(B)].
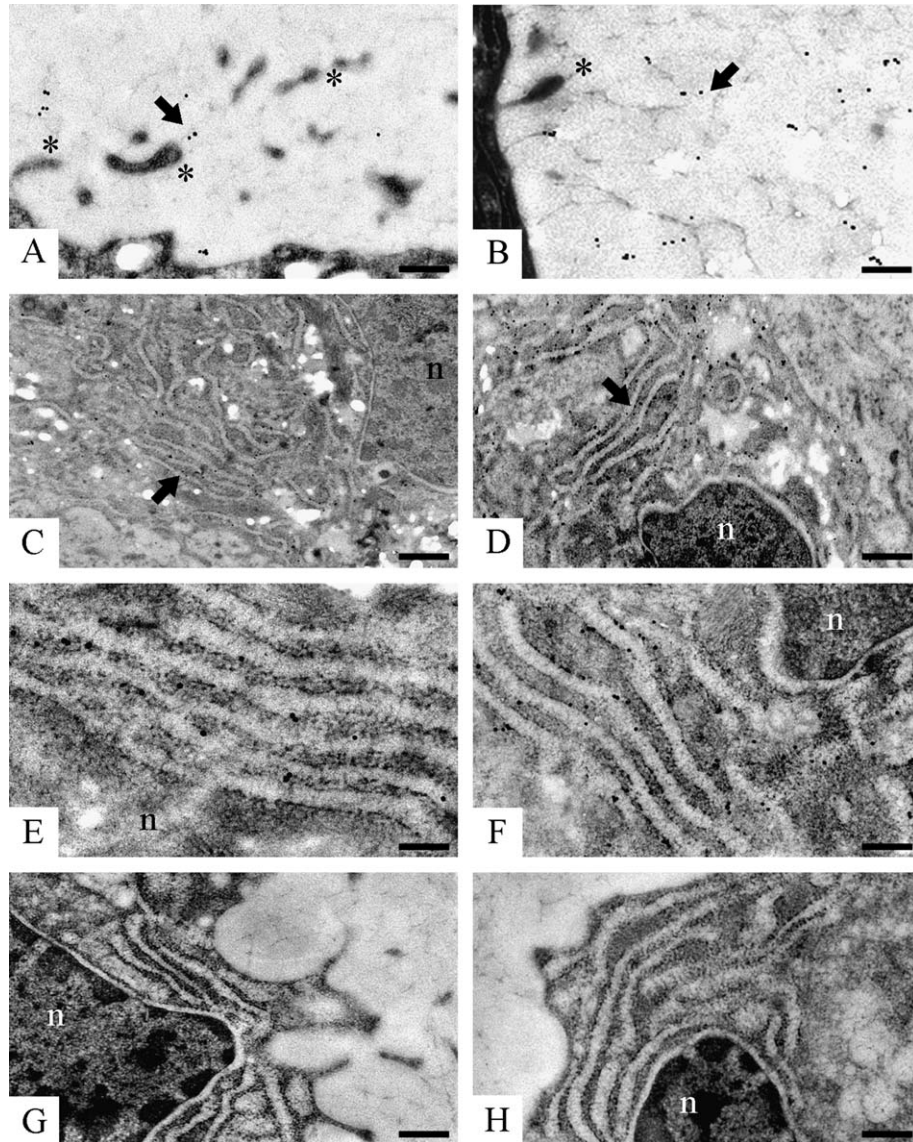
Fig. 5. Immunogold histochemistry for perlecan protein (A, B) and *in situ* hybridization for perlecan mRNA (C–H) at the ultrastructural level. Type 1 cells (A, C, E, G) with multiple filopodia (asterisks in A) on the cell surface and elongated type 2 cells (B, D, F, H) with few filopodia (asterisk in B), bars = 0.15 μm, except in C and D, bar = 0.3 μm. (A) The pericellular matrix of a type 1 cell exhibits staining for perlecan. (B) Stronger staining is found for perlecan surrounding a type 2 cell. (C) Staining for perlecan mRNA in the cytoplasm of a type 1 cell (arrow). (D) Stronger labeling in a type 2 cell (arrow). (E) Higher magnification of a type 1 cell; note staining for the perlecan mRNA at the border of the rough endoplasmic reticulum. (F) Higher magnification of a type 2 cell. (G) Control hybridizations for a type 1 cell and a type 2 cell (H) with the corresponding sense probe exhibiting no reaction; n = nucleus.

CONTROLS

The control hybridizations performed with a sense probe or without any RNA probe revealed no reaction. Ultrastructural control hybridizations were carried out with a sense probe and exhibited a sparse labeling which could be regarded as unspecific background. Treatment of sections with pure gold solution as well as with gold-coupled anti-DIG antibody produced no reaction.

RT-PCR AND REAL-TIME PCR

We isolated the cartilage cells from an area adjacent to the main defect and from a macroscopically intact area and were able to separate the two cell types detected *in vivo* by their kinetics of adherence to the fibronectin substratum of the culture flask[44]. The elongated secretory type 2 cells adhered already after 10 h, while the type 1 chondrocytes needed at least 24 h for attachment. Therefore, we were able to culture type 1 and type 2 cells separately. When near confluence was reached in the first passage, we harvested the cells and isolated the RNA. RT-PCR detected a slightly thicker band for the perlecan mRNA in type 2 cells (Fig. 7, lane 2) as compared to the type 1 cells (Fig. 7, lane 1). We also performed quantitative real-time RT-PCR and were first able to determine an unregulated house-keeping gene[40,41], HPRT-1, with identical ct values of approximately 24, i.e. the same amounts of transcripts for

the type 1 and type 2 cells (Fig. 7, lanes 3 and 4). The calibrator curve obtained by the correlation of the ct values (threshold cycles) with the dilution series of the house-keeping gene exhibits a relatively low intra-test variation [Fig. 8(A)]. Real-time PCR revealed mean ct values of 20.9 for perlecan in cultured type 2 cells and of 22.1 for type 1 cells. Applying the calculations of Pfaffl[42], this corresponds to a ratio of 0.01 for type 1 cells and a ratio of 0.02 for type 2 cells and demonstrates a 50% higher level of perlecan mRNA in type 2 cells (data not shown). The validity of the PCR results was confirmed by the melting curve [Fig. 8(B)] and by sequencing the perlecan product (data not shown). Real-time PCR of the native cartilage tissue taken from the area adjacent to the main cartilage defect revealed mean ct values of 28.0 and from a macroscopically intact area of 30.1 [Fig. 8(C)]. This demonstrates a 50% higher level of perlecan mRNA in the area adjacent to the main cartilage defect taken from native tissue.

Discussion

According to a well-established grading system, our specimens were pathohistologically graded and were all found to be grades III–IV, i.e. late stages of OA[43]. The osteoarthritic cartilage samples from patients investigated here showed signs of degeneration and to a lesser extent of regeneration. As OA is based on multifactorial conditions with a complex pathogenesis[26–38,43], it is very difficult to achieve a clear histological demarcation between degenerative and regenerative changes. For electron microscopic immunohistochemistry and ultrastructural *in situ* hybridization, we exclusively investigated the deep zones of osteoarthritic cartilage, i.e. samples from the deep zones of a macroscopically intact area and an area adjacent to the main defect. In this region, where the main regeneration processes take place, we saw mainly elongated secretory
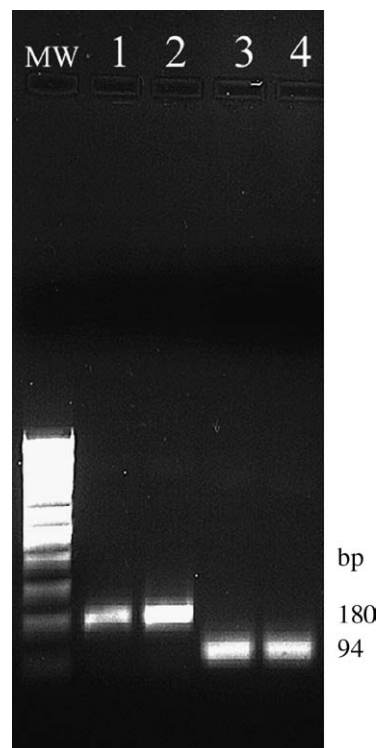

Fig. 7. Conventional RT-PCR; lane 1 shows a band for perlecan mRNA in type 1 cells, in lane 2 for perlecan in type 2 cells, lane 3 for the house-keeping gene HPRT-1 in type 1 cells and in lane 4 for HPRT-1 in type 2 cells. Note that the band in lane 1 seems to be fainter than in lane 2, but that lanes 3 and 4 exhibit a similar brightness.
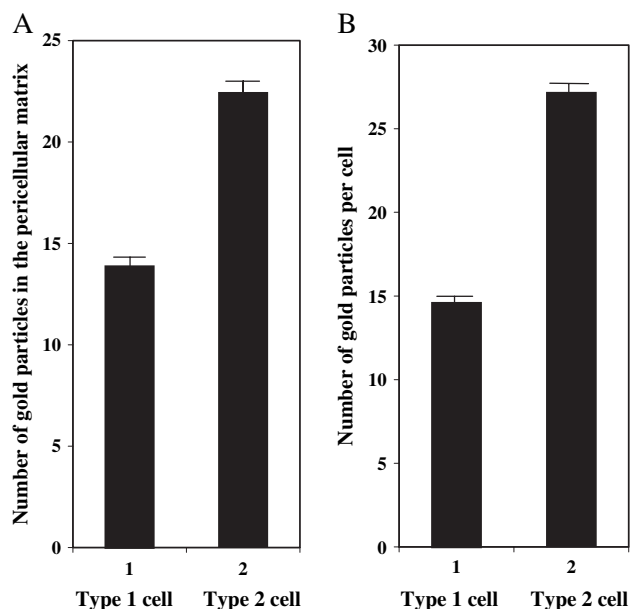

Fig. 6. (A) Mean values with S.E.M. (T on the bars) of the number of gold particles for type 1 and type 2 cells representing the amount of perlecan protein detected by immunogold histochemistry and (B) of perlecan mRNA detected by ultrastructural *in situ* hybridization.

type 2 cells described several years ago as a sign of the regeneration efforts of the diseased cartilage tissue[31,33–35].

In the present study, we investigated the role of the proteoglycan perlecan in human knee joint cartilage from patients suffering from late-stage OA. It is well known that proteoglycans such as aggrecan, biglycan and decorin are involved in the pathophysiology of OA[26–29]. A loss of decorin and biglycan was described for the superficial layers of osteoarthritic cartilage[29], while an increased amount of these proteoglycans, as well as an increased transcription rate, was detected in the deeper zones of osteoarthritic cartilage. In spite of the overall proteoglycan loss due to the reduction of the major matrix component aggrecan in late-stage OA, we also detected increasing amounts of mRNA of decorin and biglycan in the deep zones of OA cartilage. Especially the elongated secretory type 2 cells occurring in late-stage OA revealed an up-regulated expression of these proteoglycans[34].

Our present *in vivo* analysis at the light and electron microscopic level revealed a tissue distribution for perlecan in late stages of OA similar to that described for physiological cartilage[13,15,16]. Perlecan was mainly found in the deeper zones of the cartilage and in cell clusters of late stages of OA. In contrast to normal cartilage, the tissue samples taken from the area adjacent to the main defect also revealed staining for perlecan in the interterritorial matrix, where it was mainly found on fine collagen fibers.
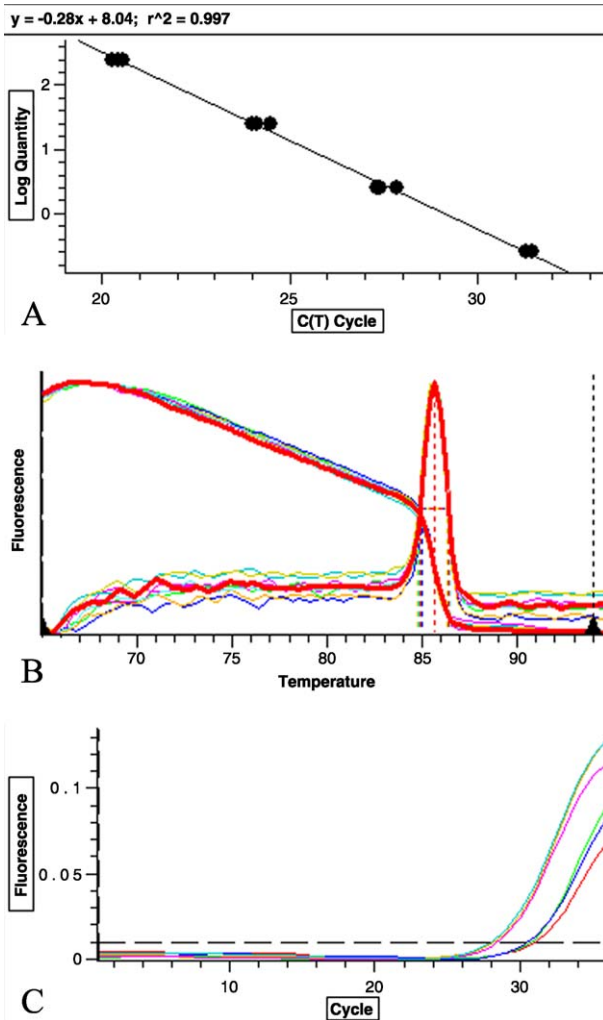
Fig. 8. Quantitative real-time RT-PCR data. (A) The calibrator curve obtained by the correlation of the ct values (threshold cycles) with the dilution series of the house-keeping gene HPRT-1. (B) Melting curve for perlecan PCR; the one peak at 86°C for all PCR runs represents the perlecan product and indicates no other transcripts. (C) Increasing intensity of fluorescence per PCR cycle for native cartilage tissue; note that the slopes of the graphs, each color representing one PCR reaction, are similar and that the thresholds for RNA isolated from the area adjacent to the main cartilage defect lie around 28 cycles (first group of curves) and from the macroscopically intact area lie around 30 cycles (second group of curves).

Perlecan knockout mice exhibited reduced amounts of collagen fibers and a lack of the typical collagen network[19] suggesting an important role of this proteoglycan in maintaining the collagen network in articular cartilage. Thus, one might assume that the increased levels of perlecan protein in late stages of OA can be seen as an effort on the part of the cartilage tissue to stabilize the extracellular matrix and the collagen fibers embedded in it. Ultrastructural analysis revealed an approximately 45% higher mRNA level for perlecan in late stages of OA. Similar observations have been made for the mRNA levels of the two small proteoglycans decorin and biglycan in late stages of OA[34]. The increase in the level of perlecan protein and mRNA is achieved by the elongated secretory type 2 cells

and these cells deposit perlecan mainly in the pericellular matrix. This was confirmed by a 50% increase of perlecan mRNA *in vivo* taken from native cartilage and *in vitro* taken from cultured cells as shown by quantitative real-time RT-PCR. With regard to the enhanced level of perlecan protein around chondrocyte clusters adjacent to the cells in the pericellular matrix, it remains to be seen whether perlecan shows any mitogenic activity in these late disease stages. The glycosaminoglycan side chains of perlecan act as a low-affinity co-receptor for FGFs and mitogenic activity has already been shown for other cells[20]. The type 2 cells which are the only new cells emerging at late stages of OA and the ones mainly responsible for the regeneration processes of cartilage matrix[33,34] produce more perlecan, which might be beneficial for the matrix integrity and the chondrocytes embedded in it. In normal cartilage, perlecan interacts with other adhesive extracellular macromolecules to stabilize the matrix and to enable the adhesion of chondrocytes to their own substratum[13,18,19]. The role of collagen type IX, which also shows characteristics of a proteoglycan, for the structural integrity of the pericellular matrix has been underlined[3]. In late stages of OA the integrity of the pericellular matrix is altered and it would be interesting to investigate whether the increased amounts of perlecan shown here can help to stabilize the pericellular matrix. The increased amount of perlecan protein, especially in the area next to the main defect, may be seen as an effort on the part of the cartilage tissue to compensate for the rapid loss of other matrix molecules such as aggrecan[29].

In conclusion, the results presented here indicate the involvement of perlecan in the pathogenesis of late stages of OA. The higher level of perlecan mRNA especially in the elongated secretory type 2 cells mainly found in the areas adjacent to the main cartilage defect and the increased level of perlecan protein mainly deposited in the pericellular matrix and to a lesser extent in the interterritorial matrix, might reflect an attempt on the part of the cartilage tissue to stabilize and protect the remaining matrix of late-stage osteoarthritic cartilage from further destruction.

References

1. Kuettner KE. Biochemistry of articular cartilage in health and disease. Clin Biochem 1992;25:155−63.
2. Morris NP, Keene DR, Horton WA. Morphology and chemical composition of connective tissue: cartilage. In: Royce PM, Steinmann B, Eds. Connective Tissue and its Heritable Disorders. Molecular, Genetic, and Medical Aspects. 2nd edn.. Wiley-Liss 2002;41−65.
3. Poole CA. Articular cartilage chondrons: form, function and failure. J Anat 1997;191:1−13.
4. Muir H. The chondrocyte, architect of cartilage. Biomechanics, structure, function and molecular biology of cartilage matrix macromolecules. BioEssays 1995; 17:1039−48.
5. Mayne R, Brewton RG. New members of the collagen superfamily. Curr Opin Cell Biol 1993;5:883−90.

6. von der Mark K. Structure, biosynthesis, and gene regulation of collagens in cartilage and bone. In: Seibel MJ, Robins SP, Bilezikian JP, Eds. Dynamics of Bone and Cartilage Metabolism. Academic Press 1999;3−29.

7. Hansen U, Bruckner P. Macromolecular specificity of collagen fibrillogenesis: fibrils of collagens I and XI contain a heterotypic alloyed core and a collagen I sheath. J Biol Chem 2003;278:37352−9.

8. Hardingham TE, Fosang AJ. Proteoglycans: many forms and many functions. FASEB J 1992;6:861−70.

9. Iozzo RV. Matrix proteoglycans: from molecular design to cellular function. Annu Rev Biochem 1998;67:609−52.

10. Doege KJ. Aggrecan. In: Kreis T, Vale R, Eds. Guidebook to the Extracellular Matrix, Anchor and Adhesion Proteins. Oxford: Oxford University Press 1999;359−61.

11. Knudson CB, Knudson W. Cartilage proteoglycans. Semin Cell Dev Biol 2001;12:69−78.

12. Heinegard D, Saxne T, Lorenzo P. Noncollagenous proteins: glycoproteins and related proteins. In: Seibel MJ, Robins SP, Bilezikian JP, Eds. Dynamics of Bone and Cartilage Metabolism. Academic Press 1999; 59−69.

13. SundarRaj N, Fite D, Ledbetter S, Chakravarti S, Hassell JR. Perlecan is a component of cartilage matrix and promotes chondrocyte attachment. J Cell Sci 1995;108:2663−72.

14. Hassell JR, Robey PG, Barrach HJ, Wilczek J, Rennard SI, Martin GR. Isolation of a heparan sulfate-containing proteoglycan from basement membrane. Proc Natl Acad Sci U S A 1980;77:4494−8.

15. Arikawa-Hirasawa E, Wilcox WR, Yamada Y. Dyssegmental dysplasia Silverman−Handmaker type: unexpected role of perlecan in cartilage development. Semin Med Genet 2001;106:254−7.

16. Melrose J, Smith S, Knox S, Whitelock J. Perlecan, the multidomain HS-proteoglycan of basement membranes, is a prominent pericellular component of ovine hypertrophic vertebral growth plate and cartilaginous endplate chondrocytes. Histochem Cell Biol 2002;118: 269−80.

17. Brown JC, Sasaki T, Gohring W, Yamada Y, Timpl R. The C-terminal domain V of perlecan promotes beta1 integrin-mediated cell adhesion, binds heparin, nidogen and fibulin-2 and can be modified by glycosaminoglycans. Eur J Biochem 1997;250:39−46.

18. Hassell J, Yamada Y, Arikawa-Hirasawa E. Role of perlecan in skeletal development and diseases. Glycoconj J 2002;19:263−7.

19. Costell M, Gustafsson E, Aszodi A, Morgelin M, Bloch W, Hunziker E, et al. Perlecan maintains the integrity of cartilage and some basement membranes. J Cell Biol 1999;147:1109−22.

20. Aviezer D, Hecht D, Safran M, Eisinger M, David G, Yayon A. Perlecan, basal lamina proteoglycan, promotes basic fibroblast growth factor-receptor binding, mitogenesis, and angiogenesis. Cell 1994;79: 1005−13.

21. Arikawa-Hirasawa E, Watanabe H, Takami H, Hassell JR, Yamada Y. Perlecan is essential for cartilage and cephalic development. Nat Genet 1999;23:354−8.

22. French MM, Smith SE, Akanabi K, Sanford T, Hecht J, Farach-Carson MC, et al. Expression of the heparan sulfate proteoglycan, perlecan, during mouse embryo-genesis and perlecan chondrogenic activity in vitro. J Cell Biol 1999;145:1103−15.

23. Murdoch AD, Dodge GR, Cohen I, Tuan RS, Iozzo RV. Primary structure of the heparan sulfate proteoglycan from basement membrane (HSPG2/perlecan). A chimeric molecule with multiple domains homologous to the low density lipoprotein receptor, laminin, neural cell adhesion molecules, and epidermal growth factor. J Biol Chem 1992;267:8544−57.

24. French MM, Gomes RR Jr., Timpl R, Hook M, Czymmek K, Farach-Carson MC, et al. Chondrogenic activity of the heparan sulfate proteoglycan perlecan maps to the N-terminal domain I. J Bone Miner Res 2002;17:48−55.

25. Arikawa-Hirasawa E, Le AH, Nishino I, Nonaka I, Ho NC, Francoma CA, et al. Structural and functional mutations of the perlecan gene cause Schwartz−Jampel syndrome, with myotonic myopathy and chondrodysplasia. Am J Hum Genet 2002;70: 1368−75.

26. Poole AR. An introduction to the pathophysiology of osteoarthritis. Front Biosci 1999;4:D662−70.

27. von der Mark K, Gluckert K. Biochemical and molecular biological aspects for the early detection of human arthrosis. Orthopaede 1990;19:2−15.

28. Buckwalter JA, Mankin HJ. Articular cartilage: degeneration and osteoarthritis, repair, regeneration, and transplantation. Instr Course Lect 1998;47: 487−504.

29. Poole AR, Rizkalla G, Ionescu M, Reiner A, Brooks E, Rorabeck C, et al. Osteoarthritis in the human knee: a dynamic process of cartilage matrix degradation, synthesis and reorganization. Agents Actions Suppl 1993;39:3−13.

30. Aigner T, Stoss H, Weseloh G, Zeiler G, von der Mark K. Activation of collagen type II expression in osteoarthritic and rheumatoid cartilage. Virchows Arch B Cell Pathol Incl Mol Pathol 1992;62:337−45.

31. Aigner T, McKenna L. Molecular pathology and pathobiology of osteoarthritic cartilage. Cell Mol Life Sci 2002;59:5−18.

32. Sandell LJ, Aigner T. Articular cartilage and changes in arthritis. An introduction: cell biology of osteoarthritis. Arthritis Res 2001;3:107−13.

33. Kouri JB, Jimenez SA, Quintero M, Chico A. Ultrastructural study of chondrocytes from fibrillated and non-fibrillated human osteoarthritic cartilage. Osteoarthritis Cartilage 1996;4:111−25.

34. Bock HC, Michaeli P, Bode C, Schultz W, Kresse H, Herken R, et al. The small proteoglycans decorin and biglycan in human articular cartilage of late-stage osteoarthritis. Osteoarthritis Cartilage 2001;9:654−63.

35. Miosge N, Waletzko K, Bode C, Quondamatteo F, Schultz W, Herken R. Light and electron microscopic in-situ hybridization of collagen type I and type II mRNA in the fibrocartilaginous tissue of late-stage osteoarthritis. Osteoarthritis Cartilage 1998;6:278−85.

36. Martel-Pelletier J. Pathophysiology of osteoarthritis. Osteoarthritis Cartilage 1999;6:371−3.

37. Gardner DL. Problems and paradigms in joint pathology. J Anat 1994;184:465−76.

38. Altman R, Asch E, Bloch D, Bole G, Borenstein D, Brandt K, et al. Development of criteria for the classification and reporting of osteoarthritis. Classification of osteoarthritis of the knee. Diagnostic and Therapeutic Criteria Committee for the American

Rheumatism Association. Arthritis Rheum 1986;29: 1039−49.

39. Miosge N, Flachsbart K, Goetz W, Schultz W, Kresse H, Herken R. Light and electron microscopical immunohistochemical localization of the small proteoglycan core proteins decorin and biglycan in human knee joint cartilage. Histochem J 1994;26: 939−45.

40. Vandesompele J, De Preter K, Pattyn F, Poppe B, Van Roy N, De Paepe A, et al. Accurate normalization of real-time quantitative RT-PCR data by geometric averaging of multiple internal control genes. Genome Biol 2002;3: [RES0034].

41. Bustin SA. Quantification of mRNA using real-time reverse transcription (RT-PCR): trends and problems. J Mol Endocrinol 2002;29:23−39.

42. Pfaffl MW. A new mathematical model for relative quantification in real-time RT-PCR. Nucleic Acids Res 2001;29:e45.

43. Collins DH, McElligott TF. Sulphate (35SO4) uptake by chondrocytes in relation to histological changes in osteoarthritic human articular cartilage. Ann Rheum Dis 1960;19:318−30.

44. Hewitt AT, Kleinman HK, Pennypacker JP, Martin GR. Identification of an adhesion factor for chondrocytes. Proc Natl Acad Sci U S A 1980;77:385−8.